Interaction of Mre11 and Rad50: Two Proteins Required for DNA Repair and Meiosis-Specific Double-Strand Break Formation in *Saccharomyces cerevisiae*

Katsuki Johzuka and Hideyuki Ogawa

Department of Biology, Faculty of Science, Osaka University, Toyonaka, Osaka 560, Japan

Manuscript received August 1, 1994
Accepted for publication January 10, 1995

ABSTRACT

A temperature-sensitive *mre11–1* mutation of *Saccharomyces cerevisiae* causes defects in meiotic recombination and DNA repair during vegetative growth at a restrictive temperature. We cloned the *MRE11* gene and found that it encodes a 643-amino acid protein with a highly acidic region containing a heptad repeat of Asp at its C-terminus and is located downstream of *YMR44* near the *RNA1* locus on the right arm of chromosome *XIII*. Transcripts of the *MRE11* gene increased transiently and showed the same kinetics as that of the *RAD50* gene during meiosis. In a *mre11* disruption mutant (*mre11*::*hisG*), meiosis-specific double-strand break (DSB) formation is abolished. A comparison of the properties of *mre11*::*hisG* and a *rad50* deletion mutant (*rad50*Δ) indicated that both mutants exhibited similar phenotypes in both meiosis and mitosis. Characterization of two double mutants, *mre11*::*hisG rad50*Δ and *mre11*::*hisG rad50S*, showed that *MRE11* and *RAD50* belong to the same epistasis group with respect to meiotic DSB formation and mitotic DNA repair. Using a two-hybrid system, we found that Mre11 interacts with Rad50 and itself *in vivo*. These results suggest that Mre11 and Rad50 proteins work in a complex in DSB formation and DNA repair during vegetative growth.

A temperature-sensitive *mre11–1* mutant was isolated as a meiotic recombination-defective strain of *Saccharomyces cerevisiae* by monitoring interchromosomal recombination in both the *his4* and *leu2* loci using a haploid strain that is disomic for chromosome *III* (AJIMURA *et al.* 1993). During meiosis, the homozygous *mre11–1* strain is deficient in inter- and intragenic recombination and forms inviable spores at a restrictive temperature. However, the spore viability of this mutant can be rescued by a *spo13* mutation that bypasses reductional division (meiosis I) and undergoes only equational division (meiosis II) (KLAPHOLZ and ESPOSITO 1980a,b). This property suggests that *MRE11* functions during the early stage(s) of meiotic recombination. In contrast, during vegetative growth, the *mre11–1* mutant is proficient in mitotic recombination and has a hyper-Rec property in interchromosomal recombination. Furthermore, the *mre11–1* mutant is sensitive to methyl methanesulfonate (MMS) at a restrictive temperature, which indicates that *MRE11* is required for DNA repair during vegetative growth.

Another mutation in *S. cerevisiae* that has been well characterized and exhibits phenotypes similar to those of *mre11–1* involves the *RAD50* gene. The mutant, *rad50*, was first identified in a strain that exhibits severe sensitivity to ionizing radiation (GAME and MORTIMER 1974). The *rad50* deletion mutants (*rad50*Δ) exhibit a hyper-Rec phenotype for both inter- and intrachromosomal recombination (ALANI *et al.* 1990; MALONE *et al.* 1990) during vegetative growth. Furthermore, meiotic recombination is completely eliminated in the *rad50*Δ mutant, resulting in inviable spore formation (GAME *et al.* 1980; RESNICK 1987; ALANI *et al.* 1990). However, its spore viability can be rescued by a *spo13* mutation (MALONE and ESPOSITO 1981). In addition, *rad50*Δ mutant is completely deficient in the formation of meiosis-specific double-strand breaks (DSBs), which is thought to be an event that initiates meiotic recombination (NICOLAS *et al.* 1989; SUN *et al.* 1989; CAO *et al.* 1990; SCHULTES and SZOSTAK 1990; GOLDWAY *et al.* 1993). Thus, the meiotic and mitotic properties of the *rad50*Δ mutant are very similar to those of *mre11–1* mutant. Interestingly, a mutant of a third gene, *XRS2*, which was originally isolated in an X-ray-sensitive strain of *S. cerevisiae* (SUSLOVA 1969 cited in IVANOV *et al.* 1992), exhibits similar properties to *rad50*Δ (IVANOV *et al.* 1992). It would appear that the *MRE11*, *RAD50* and *XRS2* genes are involved similarly in DNA repair and meiotic recombination.

A nonnull, recessive mutant of the *RAD50* gene, *rad50S*, exhibits some different phenotypes from the *rad50*Δ mutant (ALANI *et al.* 1990). During vegetative growth, the *rad50S* mutant exhibits resistance to MMS and its spontaneous recombination frequency is close to that of the wild-type strain. Therefore, the mitotic properties of the *rad50S* and wild-type strains are indistinguishable. During meiosis, although the *rad50S* mutant is capable of generating DSBs, it is deficient in DSB processing. In a wild-type strain, DSBs are processed immediately, by producing 3′-overhanging termini

Corresponding author: Hideyuki Ogawa, Department of Biology, Faculty of Science, Osaka University, Machikaneyama-chyo 1–1, Toyonaka, Osaka 560, Japan.

(SUN *et al.* 1991), which are repaired thereafter, whereas in the *rad50S* mutant, discrete DSB signals accumulate. Therefore, in the *rad50S* mutant, the progression through the meiotic recombination pathway is blocked immediately *after* DSBs formation. The properties of *rad50S* mutant suggest that *RAD50* functions at multiple steps in the meiotic recombination pathway and that mitotic DNA repair and meiotic functions can be separated.

In this work, to gain information about the *MRE11* gene and examine the relationship between *MRE11* and *RAD50,* we isolated the *MRE11* gene and constructed a *mre11* disruption mutant (*mre11*::*hisG*) and two double mutants, *mre11*::*hisG rad50*Δ and *mre11*::*hisG rad50S*. Comparative analyses using these two double mutants indicated that the two genes are in the same epistasis group with respect to both mitotic DNA repair and meiotic recombination pathways. Additional observations provided evidence that the Mre11 protein interacts with the Rad50 protein as well as with itself *in vivo*. These results suggest that Mre11 and Rad50 proteins work in a complex in the mitotic DNA repair and meiotic recombination pathways.

MATERIALS AND METHODS

Plasmids: The initial isolate of the *mre11* complementing plasmid, pKJ1101, contains a genomic 4.3-kb *Bam*HI fragment inserted at the *Bam*HI site of YRp7, and pKJ1102-pKJ1105 are derivatives of pKJ1101 with deletions in their 4.3-kb *Bam*HI fragments (Figure 1). Plasmid pKJ1107 was constructed by digestion at the *Acc*I site, treatment of its ends with the Klenow enzyme and self-ligation, which resulted in a two-base insertion at the *Acc*I site. Plasmid pNKY51 contains the *URA3* gene flanked by direct repeats of the *Salmonella hisG* DNA (ALANI *et al.* 1987). These *hisG* repeats allow the precise deletion of the *URA3* marker after transformation-mediated gene disruption. Plasmid pKJ1112-S contains a *Bam*HI fragment that is disrupted by the *hisG-URA3-hisG* fragment of pNKY51 at the *Stu*I site (Figure 1) and was used to construct the *mre11*::*hisG-URA3-hisG* mutant strain. This disruption mutation is referred to *mre11*::*hisG*. Plasmid pNKY291 (CAO *et al.* 1990) contains a 1.5-kb *Pst*I-*Eco*RI fragment derived from the downstream region of *HIS4* and was used to detect DSBs. Plasmid pNKY396 contains the *RAD50* gene with a site-directed mutation in the first ATG creating a *Nde*I recognition sequence (provided by W. RAYMOND and N. KLECKNER). Plasmid pBTM116 contains a full-length *Escherichia coli* lexA coding sequence fused to the *ADH1* promoter and the *TRP1* gene as a transformation marker and pGAD10 contains a copy of the *GAL4* acidic domain (amino acids 768–881) fused to the *ADH1* promoter and the *LEU2* gene as a transformation marker (both these plasmids were provided by P. BARTEL and S. FIELDS). The construction of each hybrid plasmid for the interaction assay using a two-hybrid system is summarized in Figure 7. Plasmid pLexA-RAD50NN contains the *Nde*I-*Nde*I fragment; it was prepared using pNKY396 and end-filled using the Klenow enzyme at the *Sma*I site of pBTM116. Plasmid pLexA-RAD50BB and pLexA-RAD50PB contain the *Bgl*II-*Bam*HI and *Pvu*II-*Bam*HI fragments of pNKY396 at the *Bam*HI and *Sma*I-*Bam*HI sites of pBTM116, respectively. Plasmid pGal4-RAD50BB contains the *Bgl*II-*Bam*HI fragment of pNKY396 inserted at the *Bam*HI site of pGAD10. The *Nde*I-*Nru*I fragment-containing pLexA-MRE11NN was prepared using pKJT7–10 (a *Nde*I site was introduced at the first ATG of the *MRE11* gene by site-directed mutagenesis) and end-filled by the Klenow enzyme at the *Sma*I site of pBTM116; pLexA-MRE11rev contains the same fragment at the *Sma*I site of pBTM116 but in the opposite direction, as pLexA-MRE11NN. Plasmid pGal4-MRE11NN contains the *Nde*I-*Nru*I fragment; it was prepared using pKJT7–10 and end-filled by the Klenow enzyme at the *Bam*HI site (this site was also end-filled by the Klenow enzyme) of pGAD10 and pGal4-MRE11SN contains the *Stu*I-*Nru*I fragment of pKJT7–10 inserted at the *Bgl*II site (this site was also end-filled by the Klenow enzyme) of pGAD10. The fusion point of each plasmid constructed was confirmed by nucleotide sequencing using the following primers: 5′-CCTTCGTC-AGCAGAGC-3′ for LexA fusions and 5′-CGATGATGAAGA-TACCC-3′ for Gal4 acidic fusions.

Yeast strains: The yeast strains used in this study are listed in Table 1. The E8–1 strain was used to clone the *MRE11* gene and N8A/E8 was used in the subcloning experiments. The NKY (provided by N. KLECKNER), SKY and KJC strains are derivatives of the SK1 strain that enters synchronously into meiosis at a high frequency (FAST 1973). The L40 (S. M. HOLLENBER, R. STERNGLANZ and H. WEINTRAUB, unpublished data) and KJ286–8a (described below) strains were used for the two-hybrid analysis.

The *mre11* disruption strain (KJC288) was constructed as follows. The diploid NKY278 strain was transformed with a 8.1-kb *Bam*HI fragment prepared from pKJ1112-S. The Ura$^+$ transformants were selected and the *MRE11* gene disruption was verified by Southern blotting. The selected diploid transformant (KJC30) was sporulated, tetrad dissected and the *MAT*α Ura$^+$ MMS^s (KJC32) and *MAT***a** Ura$^+$ MMS^s (KJC31) haploid cells were selected and mated with NKY1238 and NKY1240, respectively. The resulting diploid cells were sporulated, tetrad dissected and KJC262 and KJC268 were obtained.

The *rad50*Δ mutant (KJC210) was constructed by the one-step gene disruption methods (ROTHSTEIN 1983) using a *Bgl*II-*Eco*RI fragment of pNKY83 (ALANI *et al.* 1989) and NKY278. The Ura$^+$ haploid cells of both mating types were obtained, the Ura$^-$ cells were selected (SKY15 and SKY16) by 5-fluoro-orotic acid (5-FOA) (BOEKE *et al.* 1984) and mated to create KJC210.

The *mre11*::*hisG rad50*Δ double mutant (KJC312) was constructed as follows. The *mre11* disruption strain KJC31 was mated with SKY15, the resulting diploid was sporulated, tetrad dissected and the tetrads that exhibited 2:2 segregation of Ura$^+$ MMS^s:Ura$^-$ MMS^r were selected. The mating types of these tetrads were checked and both *MAT***a** Ura$^+$ MMS^s and *MAT*α Ura$^+$ MMS^s haploids were selected. The presence of double mutations, *mre11*::*hisG* and *rad50*Δ, in these haploids was verified by Southern blotting and the complementation tests using SKY15, SKY16, KJC31 and KJC32. These haploid cells were mated to obtain KJC312.

The *mre11*::*hisG rad50S* double mutant (KJC311) was constructed as follows. Two *mre11* haploid strains, KJC262 and KJC268, were mated with two *rad50S* haploid strains, NKY1000 and 1003, respectively. The resulting diploid strains were sporulated, tetrad dissected and two haploid strains, *MAT***a** *leu2 his4X*::*LEU2-URA3 arg4-nsp mre11*::*hisG rad50KI81-URA3* and *MAT*α *leu2 his4B*::*LEU2 arg4-bgl mre11*::*hisG rad50KI81-URA3,* were selected and mated to obtain KJC311.

The KJ286–8a strain was constructed by mating L40 with NKY274, sporulation and tetrad dissection; KJ286–8a was selected for the following genetic markers: *MAT*α Leu$^-$ Trp$^-$ His$^-$ Ura$^+$ Lys$^+$ (not checked, *LYS2*::*lexA-HIS3*).

Media: All the media used in this study, except the MYPL, presporulation and sporulation media, are described in AJIMURA *et al.* (1993). The MYPL plates contained 1% yeast ex-

TABLE 1

Yeast strains

Strain	Genotype
NKY278	a *lys2 ho::LYS2 ura3* α *lys2 ho::LYS2 ura3*
NKY274	α *lys2 ho::LYS2 ura3*
NKY1238	a *lys2 ho::LYS2 leu2::hisG his4X::LUE2-URA3 ura3 arg4-nsp*
NKY1240	α *lys2 ho::LYS2 leu2::hisG his4B::LUE2 ura3 arg4-bgl*
KJC190	NKY1238 X NKY1240
NKY641	a *lys2 ho::LYS2 leu2::hisG his4X::LEU2 ura3* α *lys2 ho::LYS2 leu2::hisG his4B::LEU2 ura3*
E8-1	α *trp1 can1 ura3 cyh2 ade6 mre11-1 ade2*
N8A-2d	a *leu2 his4 trp1 mre11-1 met2 ade2*
N8A/E8	N8A-2d X E8-1
KJC30	a *lys2 ho::LYS2 ura3 mre11:hisG-URA3-hisG* α *lys2 ho::LYS2 ura3 MRE11*
KJC31	a *lys2 ho::LYS2 ura3 mre11:hisG-URA3-hisG*
KJC32	α *lys2 ho::LYS2 ura3 mre11::hisG-URA3-hisG*
KJC262	a *lys2 ho::LYS2 leu2::hisG his4X::LEU2-URA3 ura3 arg4-nsp mre11:hisG-URA3-hisG*
KJC268	α *lys2 ho::LYS2 leu2::hisG his4B::LEU2 ura3 arg4-bgl mre11::hisG-URA3-hisG*
KJC288	KJC262 X KJC268
SKY15	α *lys2 ho::LYS2 ura3 rad50::hisG*
SKY16	a *lys2 ho::LYS2 ura3 rad50::hisG*
KJC210	SKY15 X SKY16
KJC312	a *lys2 ho::LYS2 ura3 mre11::hisG-URA3-hisG rad50::hisG* α *lys2 ho::LYS2 ura3 mre11::hisG-URA3-hisG rad50::hisG*
NKY1000	α *lys2 ho::LYS2 ura3 rad50-KI81-URA3*
NKY1003	a *lys2 ho::LYS2 ura3 rad50-KI81-URA3*
KJC211	a *lys2 ho::LYS2 leu2::hisG his4X::LEU2-URA3 ura3 arg4-nsp rad50-KI81-URA3* α *lys2 ho::LYS2 leu2::hisG his4B::LEU2 ura3 arg4-bgl rad50-KI81-URA3*
KJC311	a *lys2 ho::LYS2 leu2::hisG his4X::LEU2-URA3 ura3 arg4-nsp mre11::hisG-URA3-hisG rad50-KI81-URA3* α *lys2 ho::LYS2 leu2::hisG his4B::LEU2 ura3 arg4-bgl mre11::hisG-URA3-hisG rad50-KI81-URA3*
L40	a *LYS2::lexA-HIS3 leu2 trp1 URA3::lexA-lacZ his3*
KJ286-8a	α *LYS2 leu2 trp1 URA3::lexA-lacZ his3*

tract, 2% bacto peptone, 2% lactate and 1.5% agar (MYPL was used to remove ρ^- cells), the presporulation medium (pre-SPM) contained 1% yeast extract, 2% bacto peptone and 2% potassium acetate and the sporulation medium (SPM) contained 1% potassium acetate and 0.03% raffinose.

Cloning the *MRE11* gene: The *MRE11* gene was cloned from a genomic library (YRp7 based) (ADZUMA *et al.* 1984) by complementation of the MMS sensitivity of a *mre11-1* haploid strain, E8-1, at 34°. The Trp^+ transformants were selected on SD-Trp^- plates containing 0.01% (v/v) MMS at 34°. Among 7.5×10^6 Trp^+ transformants, 2017 were also MMS^r. After testing for cosegregation of both the MMS^r and Trp^+ phenotypes in 16 Trp^+ MMS^r transformants, plasmid DNAs were isolated from them. All the plasmid DNAs isolated had an identical 4.3-kb *Bam*HI DNA fragment cloned in the YRp7 vector (Figure 1). The candidate plasmids were introduced into a homozygous *mre11-1* mutant strain, N8A/E8, and tested for their abilities to complement MMS sensitivity and the meiotic recombination defect. One of these plasmids, the properties of which were confirmed by retransformation into yeast cells, was designated pKJ1101.

DNA Sequencing of the 4.3-kb *Bam*HI fragment: The random sonication method (DEININGER 1983) was used for DNA fragmentation. The 4.3-kb *Bam*HI fragment, at a high concentration, was self-ligated and the resulting DNAs were sonicated. These random fragments (average, 1 kb) were treated with the Klenow enzyme and inserted into the *Sma*I site of M13mp19. The nucleotide sequences of these random clones were determined by the dideoxy chain termination method (SANGER *et al.* 1977) using T7 DNA polymerase (Pharmacia) and the M13 primer.

RNA purification and analysis: The total RNA from wild-type KJC190 cells was prepared as described by ELDER *et al.* (1983). Diethyl-pyrocarbonate was used as a ribonuclease inhibitor. The poly-$(A)^+$ RNA was prepared from the total RNA using an oligo-dT column (Pharmacia) and used for S1-mapping. The total RNA from meiotic cells was purified by sporulating the diploid NKY641 strain in SPM, and RNA was prepared from cells harvested at various times after transfer to SPM. In parallel, meiotic recombination between the *his4X/his4B* heteroalleles was measured to monitor the progression of meiosis by return-to-growth methods (ESPOSITO and ESPOSITO 1974). These total RNA samples were used for Northern blotting. The RNA samples were stored in 67% ethanol at −20° until required for use.

The location and orientation of the *MRE11* transcripts were determined using the S1-mapping procedure described by BERK and SHARP (1978). The ssDNA probes were constructed with the full-length and various subfragments of the 4.3-kb *Bam*HI DNA by cloning into pUC118 and pUC119 (VIEIRA and MESSING 1987). The ssDNA probe fragments used are shown in Figure 4A. The ssDNA probes and poly-$(A)^+$ RNA were hybridized at 47° for 3 hr. After S1 nuclease treatment, the samples were suspended in 20 ml TE (10 mM Tris-Cl, pH 7.5, 1 mM EDTA) solution, and aliquots (10 ml) of the samples were electrophoresed in neutral and alkaline agarose gels.

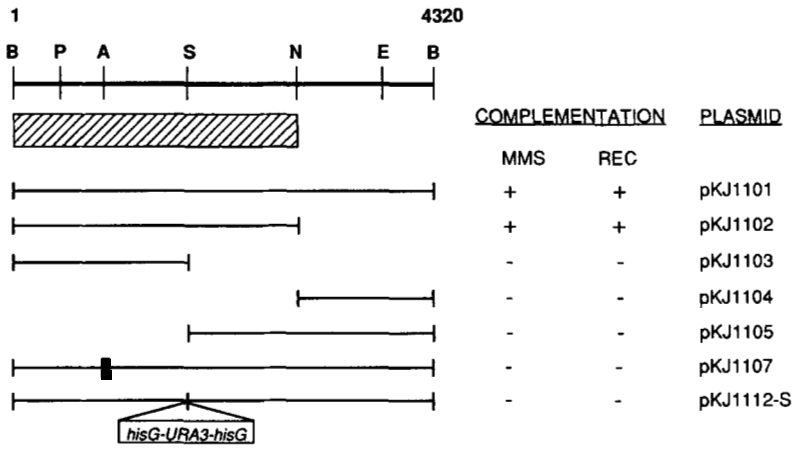

FIGURE 1.—Restriction map of the 4.3-kb *Bam*HI fragment containing the *MRE11* gene and complementation analysis of the subclones. The shaded rectangle below the map denotes the region containing the *MRE11* gene. The fragments indicated by the line were subcloned into the YRp7 vector. The results of the complementation tests for MMS sensitivity and meiotic intergenic recombination between *CAN1* and *URA3*, measured by return-to-growth methods (ESPOSITO and ESPOSITO 1974), in the *mre11-1* homozygous diploid strain (N8A/E8) at 34° are shown on the right. The solid box at the *Acc*I site of pKJ1107 represents a two base insertion created by end-filling using the Klenow fragment. In pKJ1112-S, the *hisG-URA3-hisG* (ALANI *et al.* 1987) fragment was inserted at the *Stu*I site. B, *Bam*HI; P, *Pvu*II; A, *Acc*I; S, *Stu*I; N, *Nru*I; E, *Eco*RV.

Each sample was blotted onto a nylon membrane (Millipore, GVHP304f0) and subjected to hybridization with a ^{32}P-labeled random-primed probe (FEINBERG and VOGELSTEIN 1984) prepared from the 4.3-kb *Bam*HI fragment.

To monitor the transcription of the *MRE11* and *RAD50* genes during meiosis, denatured total RNA samples were electrophoresed in formaldehyde gel, transferred to a nylon membrane, subjected to UV fixation and then hybridized with *MRE11* (*Acc*I-*Stu*I)- and *RAD50* (*Stu*I-*Pvu*II)-specific probes. The amount of each transcript was determined using a FUJIX Bio-image analyzer BAS2000 (FUJI Photo Film Co., Ltd.), and the *ACT1* signals (GALLWITZ and SEIDEL 1980) were measured in parallel to normalize the amounts of RNA in each lane.

Observation of meiosis-specific DSBs: Diploid cells (wild type, KJC190; *mre11*::*hisG*, KJC288; *rad50S*, KJC211; *mre11*::*hisG rad50S*, KJC311) grown in YPD (2 ml) were transferred into pre-SPM (200 ml) and incubated for 12 hr at 30°. Then, the cells were harvested, washed twice with SPM, suspended in SPM (200 ml) and incubated at 30°. Aliquots (15 ml) of meiotic cultures were harvested at various times after transfer to SPM and stored in 70% ethanol at −20°. The chromosomal DNA was isolated using the procedure described by CAO *et al.* (1990). Ten to 20% of the prepared DNA was digested with *Pst*I and separated on a 0.7% agarose gel using TAE buffer (SAMBROOK *et al.* 1989). The DSBs were detected by subjecting to Southern hybridization with a random-primed probe (FEINBERG and VOGELSTEIN 1984) prepared from pNKY291.

Two-hybrid analysis: The L40 and KJ286-8a strains were transformed with Gal4- and LexA-hybrid plasmids, respectively. The L40 transformants were mated with appropriate KJ286-8a transformants and the resulting diploid cells were selected on SD-Trp$^-$ Leu$^-$ plates. The protein-protein interaction was monitored by measuring the β-galactosidase activity of each diploid as described by ROSE *et al.* (1990).

RESULTS

Cloning and nucleotide sequence of the *MRE11* gene: The *MRE11* gene was isolated from a *S. cerevisiae* genomic library (ADZUMA *et al.* 1984) by complementation of the MMS sensitivity of the temperature-sensitive *mre11-1* mutant, E8-1, at 34°. All the MMS-resistant transformants carried an identical plasmid with a 4.3-kb *Bam*HI genomic fragment cloned in the YRp7 vector. A restriction map of the 4.3-kb fragment with the results of the subcloning experiments is shown in Figure 1. The subcloning experiments localized the *mre11-1* complementing activity to the 3.0-kb *Bam*HI-*Nru*I fragment. The entire 4.3-kb fragment was sequenced. Figure 2 shows the nucleotide sequence of the 3.1-kb region containing the *mre11-1* complementing activity. A long open reading frame (ORF) consisting of 1932 bp (from 812 to 2743 bp) was found in the *Bam*HI-*Nru*I region of this fragment. All the phenotypes of the disruption strain of this ORF were similar to those of *mre11-1* (under restrictive conditions), and a complementation test with the *mre11-1* mutant verified that this ORF was allelic to the *MRE11* gene and not a dominant suppressor.

The deduced Mre11 protein contained 643 amino acid residues and its molecular weight was 72,350. The DNA sequence analysis demonstrated two TATA-like sequences in the upstream region of the *MRE11* gene (TAATATATAT, 599-608, and TAATATT, 551-557) and two putative polyadenylation signals (TATAAA, 3032-3037, and AATAAA, 3103-3108) in its downstream region (Figure 2). A homology search of the deduced Mre11 protein sequence using NBRF and Swiss-Prot indicated that Mre11 is not homologous to any known protein. However, we wish to emphasize the presence of the highly acidic region containing the heptad repeat of Asp at the C-terminal region of Mre11 (Figure 2).

The nucleotide sequence from 1 to 654 in the 3.1-kb fragment was identical to that of *YMR44*, which encodes a mitochondrial ribosomal protein and is located on either chromosome *XIII* or *XVI* (MATSUSHITA *et al.* 1989). Southern blotting using the ^{32}P-labeled 4.3-kb *Bam*HI fragment by OFAGE (ROSE *et al.* 1990) indicated that the *MRE11* gene was located on chromosome *XIII* (data not shown). Measurement of the genetic intervals between *MRE11*, *RAD52* and *RNA1* on chromosome *XIII* indicated that the *MRE11* gene was mapped near *RNA1* (data not shown).

Transcription of the *MRE11* gene increases during meiosis, as does the *RAD50* gene: To determine

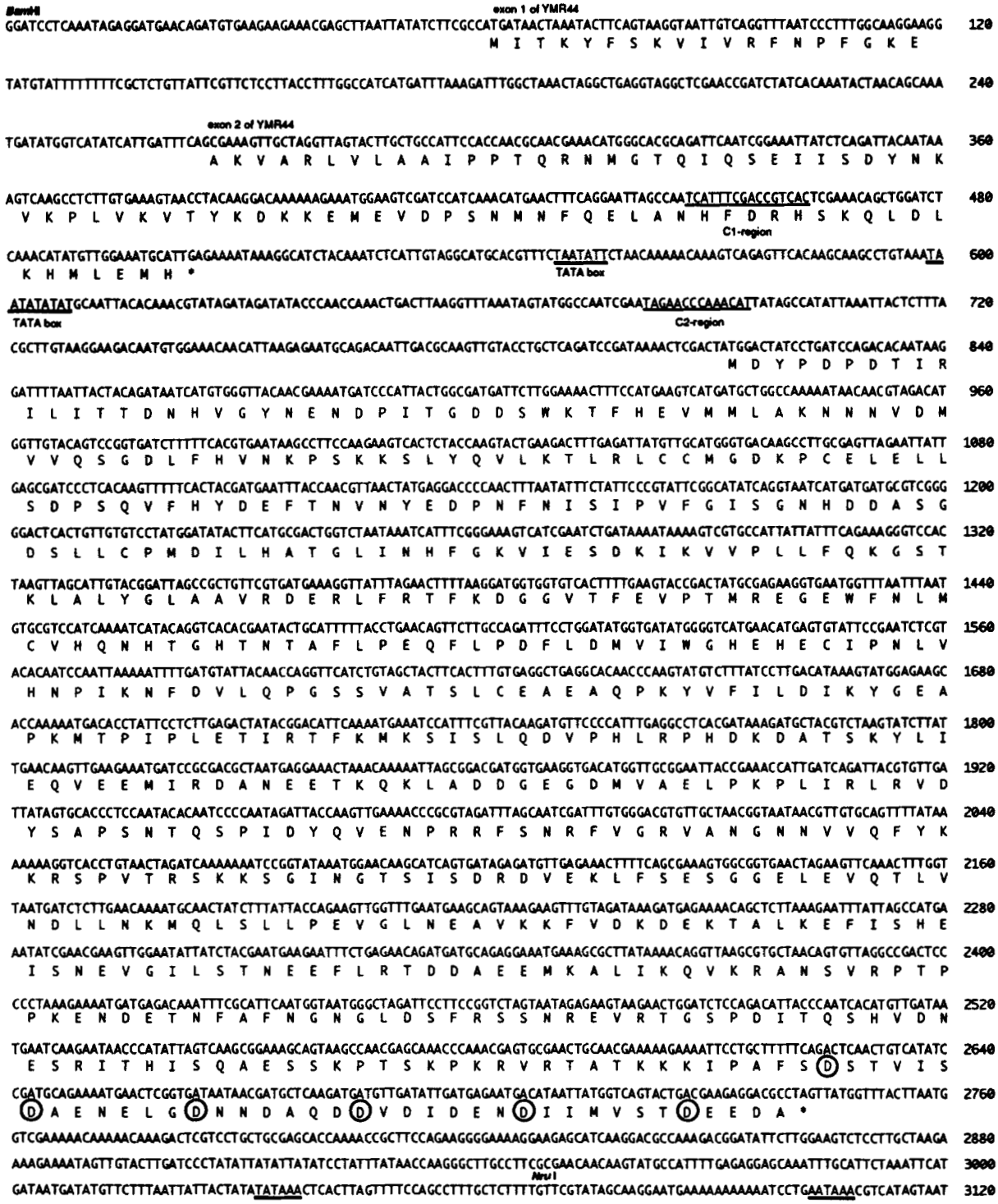

FIGURE 2.—Nucleotide sequence of a 3.1-kb region in the 4.3-kb *Bam*HI fragment. The DNA and deduced amino acid sequences of the *MRE11* gene are shown. The DNA sequence data of the 4.3-kb *Bam*HI fragment have been submitted to the GenBank, EMBL and DDBJ data bases (accession number D11463). The numbers refer to the nucleotide sequence at +1, which indicates the position of the *Bam*HI site in the 4.3-kb fragment. The TATA-like sequences located upstream of the *MRE11* ORF are underlined, as are the putative polyadenylation signals downstream of it. The C1 and C2 regions represent the sequences that are homologous with regions upstream of the *RAD50* gene (see Figure 8). The circled amino acid residues indicate the heptad repeat of Asp at the C-terminus of the Mre11 protein. The amino acid sequence in an upstream region of the *MRE11* coding region represents Ymr44 (MATSUSHITA *et al.* 1989). Therefore, the *MRE11* gene is located adjacent to the *YMR44* gene.

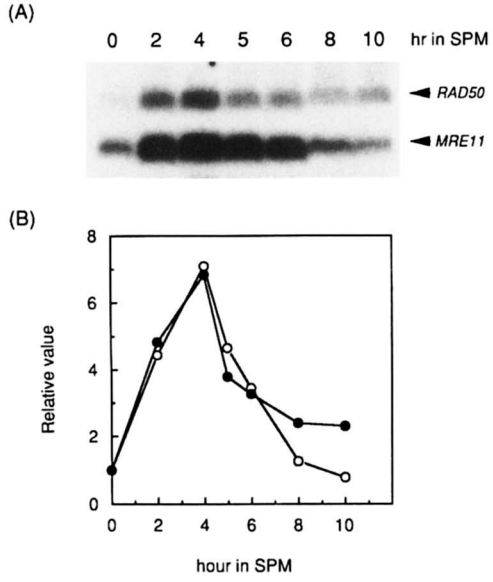

FIGURE 3.—Expression of *MRE11* and *RAD50* during meiosis. (A) Autoradiograph of Northern hybridization. The total RNA was prepared from a wild-type diploid strain (NKY641) at various times after incubation in SPM, and 10 μg total RNA was loaded onto each lane. To detect the *MRE11* RNA, a 0.94-kb *Acc*I-*Stu*I fragment prepared from pKJ1101 was labeled by the random-primer method (FEINBERG and VOGELSTEIN 1984). The *Stu*I-*Pvu*II fragment of pNKY74 (ALANI *et al.* 1989) was used as a probe for *RAD50* RNA. (B) Relative increase of *MRE11* and *RAD50* transcripts during meiosis. The signal intensity of each band was measured using a FUJIX Bio-image analyzer BAS2000 (FUJI Photo Film Co., Ltd.). The amount of each RNA per lane was normalized by dividing by that of *ACT1* RNA, which does not fluctuate during meiosis (GALLWITZ and SEIDEL 1980). ○, *MRE11* RNA; ●, *RAD50* RNA.

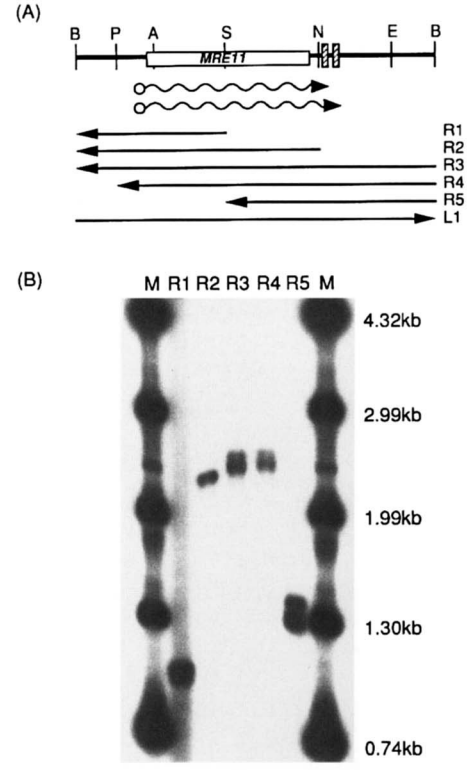

FIGURE 4.—S1-Mapping of *MRE11* transcripts. (A) The *MRE11* coding region is shown as an open box within the 4.3-kb *Bam*HI DNA fragment. The single-stranded DNAs used as probes for S1 mapping are indicated by arrows: R1, R2, R3, R4 and R5 represent anti-sense- and L1 represents sense-strand probes. The locations and orientations of the transcripts are indicated by wavy lines, and the hatched boxes located downstream of the *Nru*I site indicate polyadenylation signals. B, *Bam*HI; P, *Pvu*II; A, *Acc*I; S, *Stu*I; N, *Nru*I; E, *Eco*RV. (B) Southern hybridization analysis of S1 mapping under neutral conditions. The samples were electrophoresed on 0.8% neutral agarose gel and subjected to Southern hybridization using the 4.3-kb *Bam*HI fragment as a probe. Lane M contains size-marker DNAs prepared from the *Bam*HI fragment.

whether expression of the *MRE11* gene could be induced during meiosis, the total RNA was isolated from the wild-type diploid NKY641 strain and analyzed by Northern hybridization. A 2.5-kb RNA was detected using the *Acc*I-*Stu*I DNA fragment containing the 5′-terminal portion of the *MRE11* gene as a probe (Figure 3). The size of the RNA observed during mitosis was the same as that during meiosis. The amount of the signal in each lane was normalized using the amount of the *ACT1* signal, which remains constant during meiosis (GALLWITZ and SEIDEL 1980). Figure 3B shows the *MRE11* RNA level fluctuates during meiosis. After transfer to SPM, the amount of *MRE11* RNA increased, reached a maximum (sevenfold increase) after 4 hr and decreased thereafter.

The amount of *RAD50* RNA has also been reported to increase during meiosis (RAYMOND and KLECKNER 1993a). To compare *MRE11* and *RAD50* gene expression, the membrane was double-probed with *RAD50*- and *MRE11*-specific probes. A band of ~4.2 kb, corresponding to the *RAD50* transcript reported by RAYMOND and KLECKNER (1993a), was detected during mitosis and meiosis. The kinetics of *MRE11* and *RAD50* transcription were similar (Figure 3B). These observations suggest that transcription of these two genes may be regulated by a common mechanism.

Structure of the *MRE11* transcripts: The structure of the *MRE11* RNA was analyzed by S1 mapping. The poly-$(A)^+$ RNA was isolated from vegetative cells of a wild-type diploid strain (KJC190), hybridized with several ssDNA fragments prepared from the 4.3-kb *Bam*HI fragment (Figure 4) and digested with S1 nuclease. Figure 4B shows an autoradiograph of the fragments detected by S1 mapping under neutral conditions using the 4.3-kb *Bam*HI fragment as a probe. Two clear bands of different lengths (1.25 and 1.35 kb) were detected using the R5 anti-sense ssDNA probe, and two different-sized bands (2.3 and 2.4 kb) were also detected using the R3 (anti-sense full-length ssDNA) and R4 (anti-sense ssDNA) probes (Figure 4B). However, when R1 anti-sense ssDNA was used, only a 1.0-kb band was detected (Figure 4B). These results indicate that two mRNAs of different lengths, which originate in the same 5′-region

TABLE 2

Spontaneous mitotic recombination frequency of the *mre11::hisG*

Strain	Genotype	*his4X/his4B*	*arg4-nsp/arg4-bgl*
KJC190	*MRE11*	2.24	3.36
KJC288	*mre11::hisG*	20.4	39.9

Spontaneous mitotic interchromosomal recombination frequency was assayed in two loci using strain KJC190 and KJC288 at 30°. Each frequency ($\times 10^{-5}$) represents the average measured by three independent experiments.

and terminate at two different sites located to the right of the *Nru*I restriction site, were transcribed to the right in the 4.3-kb *Bam*HI region. Both RNAs covered the entire predicted coding region of the *MRE11* gene. It should be noted, however, that although a single band was observed with Northern blotting, two different-sized RNAs were detected by the S1-mapping method. This difference is probably attributable to the RNA length differing only by 0.1 kb, which is too small to be separated by the electrophoretic procedure used for Northern analysis. The presence of these two RNA species and their similar expression kinetics during meiosis were confirmed by the S1-mapping method using R5 ssDNA (data not shown). The same analysis was performed using alkaline agarose gel electrophoresis, which yielded the same patterns as those with neutral gel (data not shown). Therefore, we concluded that there are no introns in the *MRE11* transcripts. No bands were detected using the L1 ssDNA sense strand, which demonstrated that no anti-sense transcript longer than 0.7 kb was present (data not shown).

Construction of a *mre11* disruption mutant: The *MRE11* gene was disrupted by transforming a diploid strain with linearized pKJ1112-S (see MATERIALS AND METHODS). The tetrads exhibited four viable; however, two of them (Ura^+) formed smaller colonies than the others (Ura^-), indicating that *MRE11* is not an essential gene. However, the *mre11::hisG* mutants exhibited a slow growth phenotype. The *mre11::hisG* is recessive and is not a conditional mutation.

During vegetative growth, the spontaneous interchromosomal recombination frequency of the *mre11::hisG* mutant was 10-fold that of the wild-type strain (hyper-Rec phenotype; Table 2). During meiosis, return-to-growth experiments (ESPOSITO and ESPOSITO 1974) showed that the *mre11::hisG* mutant (KJC288) was completely deficient in induction of interchromosomal recombination (data not shown). Complete deficiency of meiotic recombination in *mre11::hisG* was also observed between CEN*III-MAT* in *mre11::hisG spo13* dyads (AJIMURA *et al.* 1993). These results indicate that the meiotic and mitotic properties of the *mre11::hisG* mutants were very similar to those of the *rad50*Δ mutants.

Analysis of meiosis-specific DSB formation in the *mre11* mutant: Site-specific DSBs with processed termini occur transiently during meiosis (SUN *et al.* 1989, 1991; CAO *et al.* 1990; GOLDWAY *et al.* 1993) and are physical landmarks of meiotic recombination. Such DSBs are considered to be initial events in meiotic recombination (NICOLAS *et al.* 1989; SCHULTES and SZOSTAK 1990; CAO *et al.* 1990; SUN *et al.* 1991). Using Southern hybridization, we attempted to ascertain the role of the *MRE11* gene in meiotic recombination by examining DSB formation at the *HIS4-LEU2* hot-spot (CAO *et al.* 1990) during meiosis in a *mre11::hisG* mutant. As shown in Figure 6, during meiosis, transient DSB signals at the *HIS4-LEU2* hot-spot were observed in the wild-type strain, whereas no DSB signals were detected in the *mre11::hisG* mutant. The same results were observed at the *ARG4* locus (data not shown). These observations indicate that the *MRE11* gene is required for generating DSB at hot-spots during meiotic recombination, as demonstrated for *RAD50, XRS2* and *SPO11* (ALANI *et al.* 1990; IVANOV *et al.* 1992).

The *MRE11* and *RAD50* genes belong to the same epistasis group: The phenotypes of the *mre11::hisG* mutant resembled those of the *rad50*Δ mutant in both meiosis and mitosis. To establish the epistasis relationship between them, we constructed *mre11::hisG rad50*Δ and *mre11::hisG rad50S* double mutants and examined their properties. Several different properties of the recessive *rad50S* mutation from *rad50*Δ and *mre11::hisG* (see the Introduction) enable epistatic analysis to be performed.

First, during vegetative growth, the MMS sensitivity of the *mre11::hisG rad50*Δ double mutant was compared with that of each single mutant (Figure 5). The MMS sensitivities of the *mre11::hisG* and the *rad50*Δ mutants were very similar. The *mre11::hisG rad50*Δ double mutant also exhibited similar sensitivity to that of each single mutant. Therefore, the *MRE11* and *RAD50* genes belong to the same epistasis group in the mitotic DNA repair pathway.

Next, the epistasis relationship between DSB formation in recombination hot-spots in these two genes during meiosis was examined. Figure 6 shows the DSB formation at the *HIS4-LEU2* hot-spot. In the wild-type strain, transient broad DSBs reflecting the processing of their termini were observed during the meiotic prophase. In contrast, in the *rad50S* mutant, discrete DSB signals were accumulated and the breaks were neither processed nor repaired, even after 12 hr in SPM (Figure 6) (ALANI *et al.* 1990). In the *mre11::hisG rad50S* double mutant, no DSB formation was detected at any time during meiosis (Figure 6). These observations indicate that *mre11::hisG* is epistatic to *rad50S* with respect to DSB formation. The sporulation frequencies were also measured. The spore formation frequency of the *mre11::hisG* mutant was reduced slightly (39% *vs.* 89% in wild type), whereas it was reduced dramatically in the *rad50S* mutant (to 0.7%). Interestingly, in the *mre11::hisG rad50S* double mutant, the spore formation

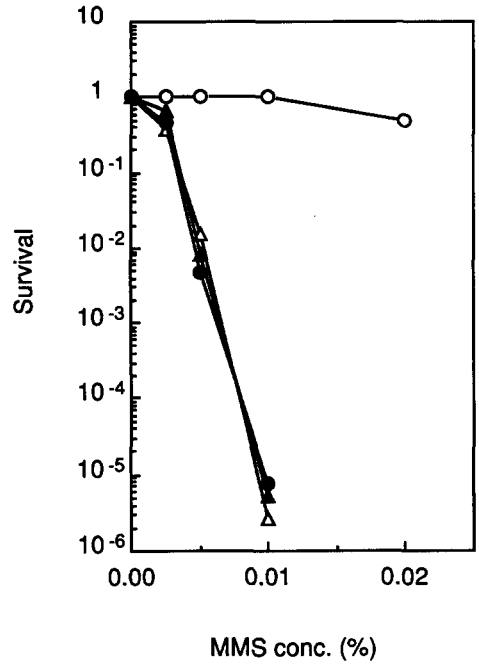

FIGURE 5.—Methyl methanesulfonate-sensitivities of wild-type and mutant strains. Homozygous diploid strains were grown to the stationary phase in liquid YPD medium at 30°. The cell cultures were diluted and plated onto complete (MYPD) plates containing various concentrations of MMS and incubated for 72 hours at 30°. ○, wild-type; △, *mre11*::*hisG*; ●, *rad50*Δ; ▲, *mre11*::*hisG rad50*Δ.

frequency recovered to the levels in the *mre11*::*hisG* or *rad50*Δ single mutants (40% and 39%, respectively). The overall meiotic and mitotic characteristics suggest that *MRE11* acts at the same, or at an earlier, step as the *RAD50* gene in mitotic DNA repair and in meiotic recombination pathways.

Physical interaction between Mre11 and Rad50 proteins: As indicated above, the *MRE11* and *RAD50* genes are genetically interactive during meiotic recombination and mitotic DNA repair. This result led us to examine the physical interaction between Mre11 and Rad50 proteins. We tested the *in vivo* interaction using a two-hybrid system (FIELDS and SONG 1989; CHIEN *et al.* 1991) in which one protein was fused to the LexA protein (full length) and the other to the Gal4 activation domain (amino acids 768–881). The L40 and KJ286–8a strains, which possess *lexA-HIS3* and *lexA-LacZ* reporter genes, were transformed with the Gal4- and LexA-fusion plasmids. The construction of each fusion plasmid is outlined in Figure 7. Both pLexA-MRE11NN and pGal4-MRE11NN were able to complement the MMS sensitivity of the *mre11* disruption mutant (data not shown), which indicates that these fusion genes encode proteins that function like the wild-type Mre11 protein.

First, the interaction between Mre11 and Rad50 proteins (Mre11-Rad50) was examined. Neither the pLexA-RAD50BB nor the pLexA-RAD50PB hybrids could activate transcription of *LacZ* in the presence of pGal4-MRE11NN. Furthermore, pLexA-RAD50NN, pLexA-RAD50BB and pLexA-RAD50PB were unable to activate transcription of *LacZ* in the presence of pGal4-MRE11SN. However, specific β-galactosidase activity was observed using pLexA-RAD50NN and pGal4-MRE11NN (Table 3). These results indicate that the Mre11 and Rad50 proteins interacted physically *in vivo*.

Second, the interaction between Mre11 proteins (Mre11-Mre11) was also examined. Using the full-length Mre11 fusion proteins, pGal4-MRE11NN and pLexA-MRE11NN, specific β-galactosidase activity was detected (Table 3). In contrast, neither the combination LexA-MRE11NN and Gal4-MRE11SN nor the combination LexA-MRE11rev and Gal4-MRE11NN activated transcription of the *LacZ* gene. These observations, together with the complementing activity of two full-length Mre11 fusions, indicate that the Mre11 protein also interacts physically with itself *in vivo*.

DISCUSSION

The *MRE11* gene of *S. cerevisiae* was isolated by complementation of the MMS sensitivity of the temperature-sensitive *mre11-1* mutant at 34°. The *MRE11* gene is located near the *RNA1* locus on chromosome *XIII* and encodes a 643-amino acid protein with a highly acidic region at its C-terminus. The level of *MRE11* RNA increases transiently during meiosis. A *mre11*::*hisG* mutant is sensitive to MMS and exhibits an interchromosomal hyper-Rec phenotype during vegetative growth. During meiosis, the *mre11*::*hisG* mutant is deficient in DSB formation at recombination hot-spots. The mitotic and meiotic properties of the *mre11*::*hisG* mutant are very similar to those of *rad50*Δ and *xrs2* (IVANOV *et al.* 1992, 1994) but differ from those of *rad51*, *rad52* (HAYNES and KUNZ 1981; SHINOHARA *et al.* 1992; OGAWA *et al.* 1994) and meiosis-specific Rec⁻ mutants (reviewed by PETES *et al.* 1991).

Regulation of *MRE11* and *RAD50* transcription: The kinetics of *MRE11* and *RAD50* transcription during meiosis were similar (Figure 3). Furthermore, two homologous sequences, C1 and C2 (Figure 8), were observed in the upstream regions of both genes and the C2 sequence was similar to the Rap1 binding site consensus sequence (ROTENBERG and WOOLFORD 1986; GRAHAM and CHAMBERS 1994). The location of these and the TATA sequences in both genes were found to be quite similar (Figure 8). These results suggest that transcription of these two genes may be controlled by a common regulatory mechanism.

Formation of a Mre11/Rad50 protein complex during DNA repair and meiotic recombination: The following four observations, taken together, suggest strongly that Mre11 and Rad50 proteins function as a protein complex in mitotic DNA repair and meiotic recombination pathways. First, the *mre11*::*hisG* and *rad50*Δ mutants exhibited quite similar properties during mitosis

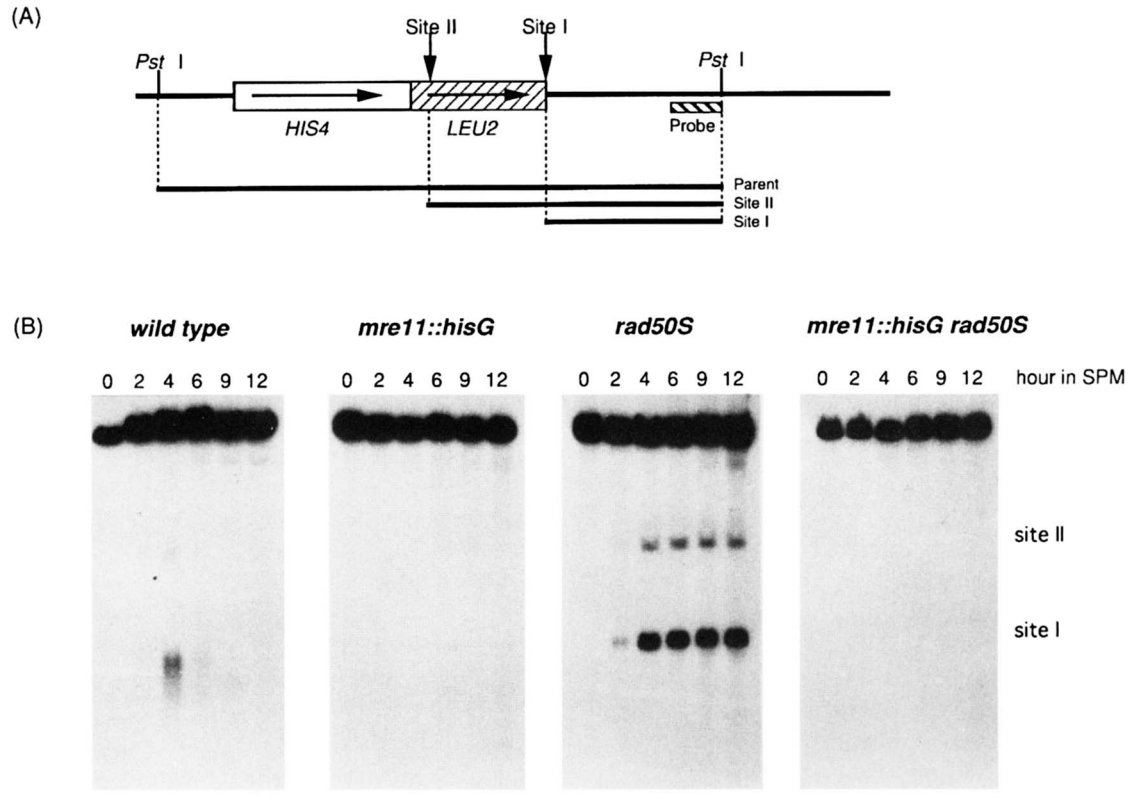

FIGURE 6.—Observation of DSBs at a meiotic recombination hot-spot. (A) Physical map of the *HIS4-LEU2* locus (CAO *et al.* 1990) on chromosome *III*. The vertical arrows indicate the sites of DSBs (sites I and II). The hatched box below the map represents the DNA fragment prepared from pNKY291 used as a probe and the horizontal lines below the map indicate the DNA fragments detected by this probe after they had been digested with *Pst*I. (B) Southern hybridization analysis of DSBs at the *HIS4-LEU2* locus in wild-type, *mre11*::*hisG*, *rad50S* and *mre11*::*hisG rad50S* strains. The times after transfer into SPM are indicated at the top of each panel. Strains used: KJC190, wild-type; KJC288, *mre11*::*hisG*; KJC211, *rad50S*; KJC311, *mre11*::*hisG rad50S*.

and meiosis: they exhibited similar MMS sensitivity, the spontaneous hyper-Rec phenotype, proficiency to carry out UV-induced recombination during vegetative growth and deficiency of DSB formation during meiotic recombination. Second, during vegetative growth, a *mre11*::*hisG rad50*Δ double mutant exhibited MMS sensitivity similar to that of each single mutant (Figure 5), which indicates both genes are involved in the same recombinational repair pathway. Third, in the *mre11*::*hisG rad50S* double mutant, no DSB signals were observed (Figure 6) and the spore formation frequency recovered to the same level as that in a *mre11*::*hisG*

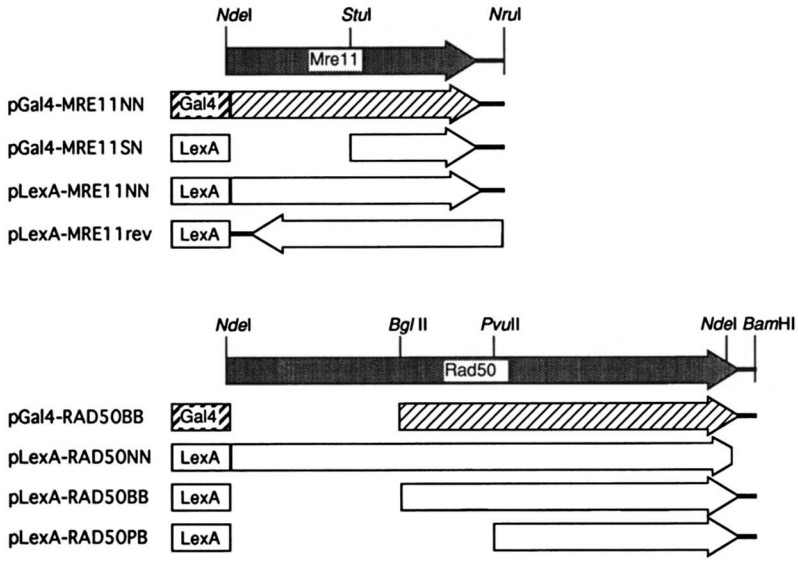

FIGURE 7.—Construction of the LexA- and Gal4-fusions (see MATERIALS AND METHODS). In pLexA-RAD50NN, the C-terminal 33 amino acids of the Rad50 protein were deleted; pBTM116 was used for LexA fusion and pGAD10 for Gal4 acidic fusion.

TABLE 3

Interaction of Mre11 and Rad50 proteins *in vivo*

LexA fusion	Gal4 acidic fusion			
	pGal4	pGal4-MRE11NN	pGal4-MRE11SN	pGal4-RAD50BB
pLexA	1.9	1.2	1.6	2.1
pLexA-MRE11NN	0.8	298	0.9	0.8
pLexA-MRE11rev	0.7	0.7	0.4	0.7
pLexA-RAD50NN	0.1	16.2	0.6	0.2
pLexA-RAD50BB	0.2	0.1	0.2	0.1
pLexA-RAD50PB	0.1	0.1	0.1	0.1

Specific activity of β-galactosidase expressed as nmol/min/mg protein is shown.

single mutant. These findings indicate that *mre11* is epistatic to *rad50S* with respect to meiotic DSB formation and sporulation. Therefore, genetic analysis of the double mutants indicated not only that the *MRE11* and *RAD50* genes work in the same pathway but also that *MRE11* acts prior to *RAD50* or they act simultaneously during the mitotic and meiotic phases. Finally, the physical interaction between Mre11 and Rad50 proteins *in vivo* was detected using a two-hybrid system (Table 3).

We also identified a Mre11-Mre11 interaction *in vivo* (Table 3). Complementation of the MMS sensitivity of a *mre11* mutant using two full-length Mre11 fusions (LexA-MRE11NN and Gal4-MRE11NN) indicated they both encoded fusion proteins that functioned like the wild-type Mre11 protein. These results suggest that Mre11 exists *in vivo* as a dimer or multimer. The biological significance of the Mre11-Mre11 interaction could be examined by isolating a dominant negative mutation of the *MRE11* gene. A similar self-interaction (Rad50-Rad50) was observed in studies using Rad50 protein purified from yeast (Raymond and Kleckner 1993b). The Rad50-Rad50 interaction is considered to be important for the function of Rad50 protein, because of its structural similarity to the myosin S-2 domain (Alani *et al.* 1989).

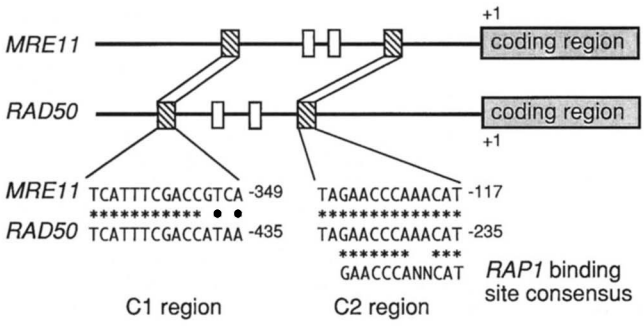

Figure 8.—The upstream homologous regions of the *MRE11* and *RAD50* genes. The hatched boxes (C1 and C2) show the homologous regions of the *MRE11* and *RAD50* genes, the open boxes indicate the TATA sequences and the numbers denote the distance (in base pair) from the corresponding first ATG. The nucleotide sequence of the *RAD50* gene is that reported by Alani *et al.* (1989). The C2 region was homologous with the Rap1 binding site consensus sequence (Rotenberg and Woolford 1986; Graham and Chambers 1994).

In the two-hybrid analysis, the deletions of N-terminal half of the Mre11 protein and of N-terminal one third of the Rad50 protein failed to make the reporter genes active (Table 3). Therefore, these regions are possible to be required for protein-protein interactions. However, we do not know yet that these truncated fusion proteins are stable or properly folded in the cells; this possibility needs further study. In addition to this possibility, we can speculate C-terminal region as one of protein-protein interaction sites. As shown in Figure 2, a highly acidic-rich region containing a heptad repeat of Asp was observed in a C-terminus of the Mre11 protein. The acidic-rich regions of yeast transcriptional activators and bacteriophage gp32 are required for protein-protein interactions (Lewin 1990; Krassa *et al.* 1991). Therefore, it is also possible that the acidic-rich region of the Mre11 protein is involved in interactions.

Other possible members of the complex: The *mre11::hisG* and *rad50*Δ mutants exhibit complex and pleiotropic phenotypes. The sensitivities of these mutants to MMS and γ-rays suggest that *MRE11* and *RAD50* are required for DSB repair (*after* DSB damage has occurred) during vegetative growth. Conversely, as no DSB formation at recombination hot-spots was observed in these mutants during meiosis, these genes would appear to be required for DSB formation *per se* in the meiotic recombination pathway (*before* DSB formation). The meiotic role of *MRE11* and *RAD50* in DSB formation may be attributable to interaction(s) with some meiosis-specific protein(s). Several meiosis-specific genes, the mutants of which are deficient in DSB formation, have been found in *S. cerevisiae* (*spo11,* Alani *et al.* 1990; *mer2,* T. Nakagawa and H. Ogawa, unpublished data; *rec114,* S.-H. Leem, N. Satoh and H. Ogawa, unpublished data). Interaction(s) between such meiosis-specific factor(s) and proteins of the Mre11/Rad50 complex may confer the ability to form DSBs during meiosis. Further investigations into possible interactions with additional meiosis-specific proteins may provide information that will help to understand the mechanism of meiotic DSB formation at recombination hot-spots.

A product of a third gene, *XRS2*, may also interact with the Mre11/Rad50 complex. The *XRS2* gene, which is known to be required for recombinational repair in *S. cerevisiae*, was also found to be required for DSB formation during meiotic recombination (IVANOV *et al.* 1992), as observed with the *mre11*::*hisG* and *rad50*Δ mutants. In addition, *XRS2* exhibits epistatic interactions with *RAD50* with respect to meiotic DSB formation and mitotic DNA repair. Therefore, the *mre11*, *rad50* and *xrs2* mutants exhibit similar phenotypes during both meiosis and vegetative growth and the Xrs2 protein is, therefore, an obvious candidate for the complex. Recently, to identify other members of the Mre11/Rad50 complex, we tried to isolate proteins that can bind to Mre11 from a yeast genomic library using the two-hybrid system and isolated Gal4-Xrs2 fusion proteins (K. JOHZUKA and H. OGAWA, unpublished data).

Model for the role of the Mre11/Rad50 complex: Two significant observations of the involvement of the chromatin structure in DSB formation and mitotic recombination frequency have been reported. First, the sites of DSB formation are hypersensitive to DNaseI or micrococcal nuclease (MNase) during not only meiosis but also vegetative growth (WU and LICHTEN 1994; OHTA *et al.* 1995), which indicates that meiotic recombination hot-spot loci are exposed sites in chromatin during both phases. Second, a *sir3* mutant exhibits the hyper-Rec phenotype during vegetative growth (PALLADINO *et al.* 1993). The *SIR3* gene is known to be required for the repression of two silent loci, *HMR* and *HML* (RINE and HERSKOWITZ 1987), and the transcriptional repression mediated by *SIR3* requires interaction with a nucleosome component, histone H4 (JOHNSON *et al.* 1990). This interaction is thought to cause a chromatin structure change, thus preventing access of the transcriptional machinery to the region. Therefore, the characteristics of *sir3* suggest that exposed sites in the chromatin are more recombinogenic than other regions that are masked by the histone octamer.

Considering the hyper-Rec properties of the *mre11*::*hisG* and *rad50*Δ mutants from the point of view of chromatin structure, the role of the Mre11/Rad50 complex may be as follows. The function of the complex is to bind the DNA at exposed sites in the chromatin and change it into some unknown structure. This might lead to repression of the production of spontaneous recombinogenic lesions, which may occur everywhere in the genome. If this is the case, the hyper-Rec properties of the *mre11*::*hisG* and *rad50*Δ mutants can be understood easily, as discussed above for the *sir3* mutant. During meiosis, as discussed above, the complexes bind to the exposed sites of chromatin and then recruit some meiosis-specific protein (*e.g.*, nuclease) to produce DSBs. The double-stranded DNA binding activities of purified Rad50 (RAYMOND and KLECKNER 1993b) and Mre11 (K. JOHZUKA and H. OGAWA, unpublished data) proteins provide support for this hypothesis.

We thank T. OGAWA and M. AJIMURA for helpful discussions, as well as Drs. N. KLECKNER, J. INSELBURG, A. SHINOHARA and R. KATO for critical reading of the manuscript. This work was supported by Grant-in-Aids for Specially Promoted Research, and for Scientific Research on Priority Areas, from The Ministry of Education, Science and Culture of Japan. K.J. was supported by a Fellowship of the Japan Society for the Promotion of Science.

LITERATURE CITED

ADZUMA, K., T. OGAWA and H. OGAWA, 1984 Primary structure of the *RAD52* gene in *Saccharomyces cerevisiae*. Mol. Cell. Biol. **4:** 2735–2744.

AJIMURA, M., S.-H. LEEM and H. OGAWA, 1993 Identification of new genes required for meiotic recombination in *Saccharomyces cerevisiae*. Genetics **133:** 51–66.

ALANI, E., L. CAO and N. KLECKNER, 1987 A method for gene disruption that allows repeated use of *URA3* selection in the construction of multiply disrupted yeast strains. Genetics **116:** 541–545.

ALANI, E., S. SUBBIAH and N. KLECKNER, 1989 The yeast *RAD50* gene encodes a predicted 153-kD protein containing a puRINE nucleotide-binding domain and two large heptad-repeat regions. Genetics **122:** 47–57.

ALANI, E., R. PADMORE and N. KLECKNER, 1990 Analysis of wild-type and *rad50* mutants of yeast suggests an intimate relationship between meiotic chromosome synapsis and recombination. Cell **61:** 419–436.

BERK, A. J., and P. A. SHARP, 1978 Spliced early mRNAs of simian virus 40. Proc. Natl. Acad. Sci. USA **75:** 1274–1278.

BOEKE, J. D., F. LACROUTE and G. R. FINK, 1984 A positive selection for mutants lacking orotidine-5′-phosphate decarboxylase activity in yeast: 5-fluoro-orotic acid resistance. Mol. Gen. Genet. **197:** 345–346.

CAO, L., E. ALANI and N. KLECKNER, 1990 A pathway for generation and processing of double-strand breaks during meiotic recombination in *Saccharomyces cerevisiae*. Cell **61:** 1089–1101.

CHIEN, C., P. L. BARTEL, R. STERNGLANZ and S. FIELDS, 1991 The two-hybrid system: a method to identify and clone genes for proteins that interact with a protein of interest. Proc. Natl. Acad. Sci. USA **88:** 9578–9582.

DEININGER, P. L., 1983 Random subcloning of sonicated DNA: application to shotgun DNA sequence analysis. Anal. Biochem. **129:** 216–223.

ELDER, R. T., E. Y. LOH and R. W. DAVIS, 1983 RNA from the yeast transposable element Tyl has both ends in the direct repeats, a structure similar to retrovirus RNA. Proc. Natl. Acad. Sci. USA **80:** 2432–2436.

ESPOSITO, R. E., and M. S. ESPOSITO, 1974 Genetic recombination and commitment to meiosis in *Saccharomyces*. Proc. Natl. Acad. Sci. USA **71:** 3172–3176.

FAST, D., 1973 Sporulation synchrony of *Saccharomyces cerevisiae* grown various carbon sources. J. Bacteriol. **116:** 925–930.

FEINBERG, A. P., and B. VOGELSTEIN, 1984 A technique for radiolabeling DNA restriction endonuclase fragments to high specific activity. Anal. Biochem. **137:** 266–267.

FIELDS, S., and O. SONG, 1989 A novel genetic system to detect protein-protein interactions. Nature **340:** 245–246.

GALLWITZ, D., and R. SEIDEL, 1980 Molecular cloning of the actin gene from yeast *Saccharomyces cerevisiae*. Nucleic Acids Res. **8:** 1043–1059.

GAME, J. C., and R. K. MORTIMER, 1974 A genetic study of X-ray sensitive mutants in yeast. Mutat. Res. **24:** 281–292.

GAME, J. C., T. J. ZAMP, R. J. BRAUN, M. RESNICK and R. M. ROTH, 1980 The role of radiation (*rad*) genes in meiotic recombination in yeast. Genetics **94:** 51–68.

GOLDWAY, M., A. SHERMAN, D. ZENVIRTH, T. ARBEL and G. SIMCHEN, 1993 A short chromosomal region with major roles in yeast chromosome *III* meiotic disjunction, recombination and double-strand breaks. Genetics **133:** 159–169.

GRAHAM, I. R., and A. CHAMBERS, 1994 Use of the selection technique to identify the diversity of binding sites for the yeast *RAP1* transcription factor. Nucleic Acids Res. **22:** 124–130.

HAYNES, R. H., and B. A. KUNZ, 1981 DNA repair and mutagenesis in yeast, pp. 371–414 in *The Molecular Biology of the Yeast Saccharo-*

myces cerevisiae: Life Cycle and Inheritance, edited by J. N. STRATHERN, E. W. JONES and J. R. BROACH. Cold Spring Harbor Laboratory, Cold Spring Habor, NY.

IVANOV, E. L., V. G. KOROLEV and F. FABRE, 1992 *XRS2,* a DNA repair gene of *Saccharomyces cerevisiae,* is needed for meiotic recombination. Genetics **132:** 651–664.

IVANOV, E. L., N. SUGAWARA, C. I. WHITE, F. FABRE and J. E. HABER, 1994 Mutations in *XRS2* and *RAD50* delay but do not prevent mating type switching in *Saccharomyces cerevisiae.* Mol. Cell. Biol. **14:** 3414–3425.

JOHNSON, L. M., P. S. KAYNE, E. S. KAHN and M. GRUNSTEIN, 1990 Genetic evidence for an interaction between *SIR3* and histone H4 in the repression of the silent mating loci in *Saccharomyces cerevisiae.* Proc. Natl. Acad. Sci. USA **87:** 6286–6290.

KLAPHOLZ, S., and R. E. ESPOSITO, 1980a Isolation of *spo12–1* and *spo13–1* from a natural variant of yeast that undergoes a single meiotic division. Genetics **96**: 567–588

KLAPHOLZ, S., and R. E. ESPOSITO, 1980b Recombination and chromosome segregation during the single division meiosis in *spo12–1* and *spo13–1* diploids. Genetics **96**: 589–611

KRASSA, K. B., L. S. GREEN and L. GOLD, 1991 Protein–protein interactions with the acidic COOH terminus of the single stranded DNA binding protein of the bacteriophage T4. Proc. Natl. Acad. Sci. USA **88**: 4010–4014.

LEWIN, B., 1990 Commitment and activation at pol II promoters: a tail of protein-protein interactions. Cell **61:** 1161–1164

MALONE, R. E., and R. E. ESPOSITO, 1981 Recombinationless meiosis in *Saccharomyces cerevisiae.* Mol. Cell. Biol. **1:** 891–901.

MALONE, R. E., T. WARD, S. LIN and J. WARING, 1990 The *RAD50* gene, a member of the double-strand break repair epistasis group, is not required for spontaneous mitotic recombination in yeast. Curr. Genet. **18:** 111–116.

MATSUSHITA, Y., M. KITAGAWA and K. ISONO, 1989 Cloning and analysis of nuclear genes for two mitochondrial ribosomal proteins in yeast. Mol. Gen. Genet. **219:** 119–124.

NICOLAS, A., D. TRECO, N. P. SCHULTES and J. W. SZOSTAK, 1989 An initiation site for meiotic gene conversion in the yeast *Saccharomyces cerevisiae.* Nature **338:** 35–39.

OGAWA, T., A. SHINOHARA, A. NABETANI, T. IKEYA, X. YU *et al.,* 1994 RecA-like recombination proteins in eukaryotes: functions and structures of *RAD51* genes. Cold Spring Harbor Symp. Quant. Biol. **58:** 567–576.

OHTA, K., T. SHIBATA and A. NICOLAS, 1995 Changes in chromatin structure at recombination initiation sites during yeast meiosis. EMBO J. **13:** 5754–5763.

PALLADINO, F., T. LAROCHE, E. GILSON, A. AXELROD, L. PILLUS *et al.,* 1993 *SIR3* and *SIR4* proteins are required for the positioning and integrity of yeast telomeres. Cell **75:** 543–555.

PETES, T. D., R. E. MALONE and L. S. SYMINGTON, 1991 Recombination in yeast, pp. 407–522 in *The Molecular and Cellular Biology of the Yeast Saccharomyces.* Vol. 1: Genome Dynamics, Protein Synthesis and Energetics, edited by J. BROACH, J. PRINGLE and E. JONES. Cold Spring Harbor Laboratory, Cold Spring Harbor, NY.

RAYMOND, W. E., and N. KLECKNER, 1993a Expression of the *Saccharomyces cerevisiae RAD50* gene during meiosis: steady-state transcript levels rise and fall while steady state protein levels remain constant. Mol. Gen. Genet. **238:** 390–400.

RAYMOND, W. E., and N. KLECKNER, 1993b *RAD50* protein of *S. cerevisiae* exhibits ATP-dependent DNA binding. Nucleic Acids Res. **21:** 3851–3856.

RESNICK, M. A., 1987 Investigating the genetic control of biochemical events in meiotic recombination, pp. 157–210 in *Meiosis,* edited by P. B. MOENS. Academic Press, New York.

RINE, J., and I. HERSKOWITZ, 1987 Four genes responsible for a position effect on expression from *HML* and *HMR* in *S. cerevisiae.* Genetics **116:** 9–22.

ROSE, M. E., F. WINSTON and P. HIETER, 1990 *Methods in Yeast Genetics: A Laboratory Course Manual.* Cold Spring Harbor Laboratory, Cold Spring Harbor, NY.

ROTENBERG, M. O., and J. L. WOOLFORD, JR., 1986 Tripartite upstream promoter element essential for expression of *Saccharomyces cerevisiae* ribosomal protein genes. Mol. Cell. Biol. **6:** 674–687.

ROTHSTEIN, R., 1983 One-step gene disruption in yeast. Methods Enzymol. **101:** 202–211.

SAMBROOK, J., E. F. FRITSCH and T. MANIATIS, 1989 *Molecular Cloning: A Laboratory Manual,* Ed. 2, Cold Spring Harbor Laboratory, Cold Spring Harbor, NY.

SANGER, F., S. NICKLEN and A. R. COULSON, 1977 DNA sequencing with chain-terminating inhibitors. Proc. Natl. Acad. Sci. USA **74:** 5463–5467.

SCHULTES, N. P., and J. W. SZOSTAK, 1990 Decreasing gradients of gene conversion on both sides of the initiation site for meiotic recombination at the *ARG4* locus in yeast. Genetics **126:** 813–822.

SHINOHARA, A., H. OGAWA and T. OGAWA, 1992 Rad51 protein involved in repair and recombination in *Saccharomyces cerevisiae* is a recA-like protein. Cell **69:** 457–470.

SUN, H., D. TRECO, N. P. SCHULTES and J. W. SZOSTAK, 1989 Double-strand breaks at an initiation site for meiotic gene conversion. Nature **338:** 87–90.

SUN, H., D. TRECO and J. W. SZOSTAK, 1991 Extensive 3′-overhanging, single-stranded DNA associated with the meiosis-specific double-strand breaks at the *ARG4* recombination initiation sites. Cell **64:** 1155–1161.

SUSLOVA, N. G., 1969 Isolation of X-ray sensitive mutants in *Saccharomyces cerevisiae.* Radiobiologia **9:** 933–936

VIEIRA, J., and J. MESSING, 1987 Production of single-stranded plasmid DNA. Methods Enzymol. **153:** 3–11.

WU, T. C., and M. LICHTEN, 1994 Meiosis-induced double-strand break sites determined by yeast chromatin structure. Science **263:** 515–518.

Communicating editor: P. J. PUKKILA